AD-A044 432 AIR FORCE ROCKET PROPULSION LAB EDWARDS AFB CALIF F/G 11/9
A MICROPHOTOGRAPHIC STUDY OF AN EPOXY BOND SYSTEM FOR SEMICONDU--ETC(U)
AUG 77 T J CHEW, D H BANASIAK

UNCLASSIFIED AFRPL-TR-77-39 NL

1 OF 1
AD
A044432

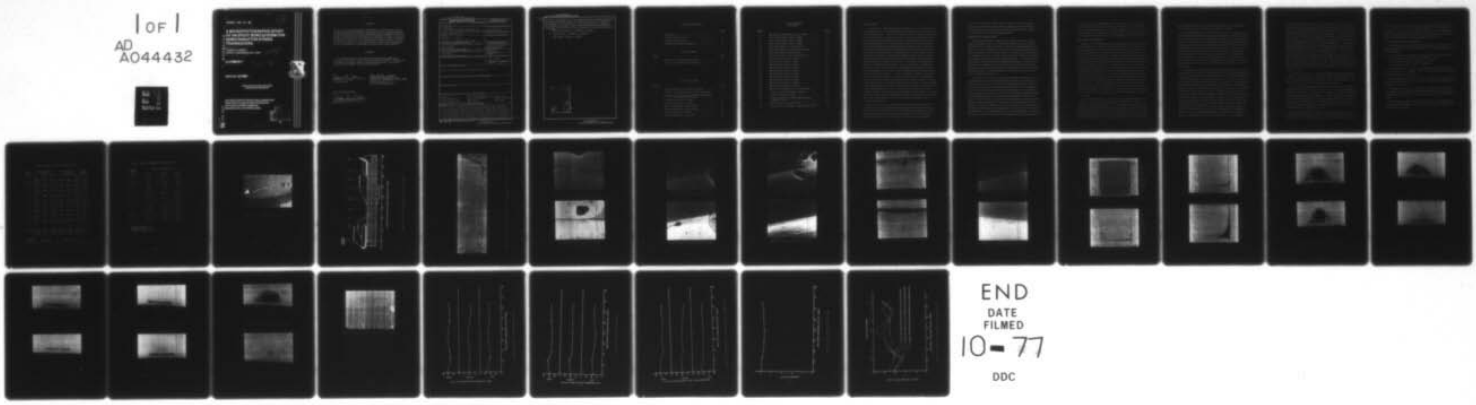

END
DATE
FILMED
10-77
DDC

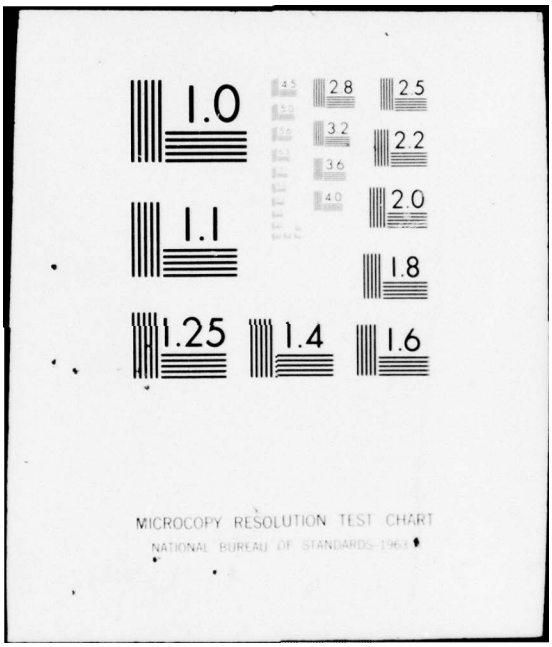
1.0
1.1
1.25
1.4
1.6
1.8
2.0
2.2
2.5
2.8
3.2
3.6
4.0
4.5
MICROCOPY RESOLUTION TEST CHART
NATIONAL BUREAU OF STANDARDS-1963

AFRPL-TR-77-39

A MICROPHOTOGRAPHIC STUDY OF AN EPOXY BOND SYSTEM FOR SEMICONDUCTOR STRESS TRANSDUCERS

THOMAS J.C. CHEW
DANIEL H. BANASIAK, CAPT, USAF

AUGUST 1977

SPECIAL REPORT

APPROVED FOR PUBLIC RELEASE;
DISTRIBUTION UNLIMITED

AIR FORCE ROCKET PROPULSION LABORATORY
DIRECTOR OF SCIENCE AND TECHNOLOGY
AIR FORCE SYSTEMS COMMAND
EDWARDS AFB, CALIFORNIA 93523

NOTICES

"When U.S. Government drawings, specifications, or other data are used for any purpose other than a definitely related government procurement operation, the Government thereby incurs no responsibility nor any obligation whatsoever, and the fact that the Government may have formulated, furnished, or in any way supplied the said drawings, specifications or other data, is not to be regarded by implication or otherwise, or in any manner licensing the holder or any other person or corporation, or conveying any rights or permission to manufacture, use or sell any patented invention that may in any way be related thereto".

FORWARD

This report has been reviewed by the Information Office/DOZ and is releasable to the National Technical Information Service (NTIS). At NTIS it will be available to the general public, including foreign nations. This report is unclassified and suitable for general public release.

Thomas J. C. Chew

THOMAS J. C. CHEW,
Project Manager

Robert R. Middleton

ROBERT R. MIDDLETON, CAPT, USAF
Chief, Surveillance and
Mechanical Behavior Section

FOR THE COMMANDER

Charles R. Cooke

CHARLES R. COOKE, Director
Solid Rocket Division

UNCLASSIFIED

SECURITY CLASSIFICATION OF THIS PAGE *(When Data Entered)*

REPORT DOCUMENTATION PAGE		READ INSTRUCTIONS BEFORE COMPLETING FORM
1. REPORT NUMBER AFRPL-TR-77-39	2. GOVT ACCESSION NO.	3. RECIPIENT'S CATALOG NUMBER
4. TITLE *(and Subtitle)* A MICROPHOTOGRAPHIC STUDY OF AN EPOXY BOND SYSTEM FOR SEMICONDUCTOR STRESS TRANSDUCERS		5. TYPE OF REPORT & PERIOD COVERED Special Report 6. PERFORMING ORG. REPORT NUMBER
7. AUTHOR(s) THOMAS J. C. CHEW DANIEL H. BANASIAK, CAPT, USAF		8. CONTRACT OR GRANT NUMBER(s)
9. PERFORMING ORGANIZATION NAME AND ADDRESS AIR FORCE ROCKET PROPULSION LABORATORY (MKPB) EDWARDS AFB, CA 93523		10. PROGRAM ELEMENT, PROJECT, TASK AREA & WORK UNIT NUMBERS Program Element 62302F Project 5730, Task 13 JON: 573013NE
11. CONTROLLING OFFICE NAME AND ADDRESS AIR FORCE ROCKET PROPULSION LABORATORY/MKPB EDWARDS AFB, CA 93523		12. REPORT DATE August 1977 13. NUMBER OF PAGES 31
14. MONITORING AGENCY NAME & ADDRESS*(if different from Controlling Office)*		15. SECURITY CLASS. *(of this report)* Unclassified 15a. DECLASSIFICATION DOWNGRADING SCHEDULE N/A

16. DISTRIBUTION STATEMENT *(of this Report)*

Approved for public release; distribution unlimited.

17. DISTRIBUTION STATEMENT *(of the abstract entered in Block 20, if different from Report)*

18. SUPPLEMENTARY NOTES

19. KEY WORDS *(Continue on reverse side if necessary and identify by block number)*

Silicon gage	Semiconductor gage thickness	Stress gage
Silicon strain gage	Epoxy bond thickness	Stress transducers
Semiconductor gage	Epoxy bond	Strain gage
Semiconductor strain gage	Gage bond system	

20. ABSTRACT *(Continue on reverse side if necessary and identify by block number)*

A specimen of epoxy bonded silicon strain gage was photographed at various angles and localities using a Quick Scanning Electron Microscope. The specimen was magnified up to 5,000 times. Epoxy fillet size variation, epoxy filler particles and metal surface texture were recorded. Relatively large dust particles were also found on the specimen surface. Consequently, an energy dispersion elemental analysis was performed on two arbitrarily selected dust particles and found that their predominant composition was →next page

DD FORM 1 JAN 73 1473 EDITION OF 1 NOV 65 IS OBSOLETE

UNCLASSIFIED

SECURITY CLASSIFICATION OF THIS PAGE *(When Data Entered)*

Cont.

aluminum. The specimen was then ground in successive planes perpendicular to the length of the silicon gage. Ten such specimen cross-sections were photographed at 500X magnification. These photographs were analyzed for the magnitude and variation of epoxy thickness, gage thickness and gage width. The average values for these parameters were found to be as follows:

1. Epoxy layer thickness = 0.000498" ± 0.000067"
2. Gage thickness = 0.000449" ± 0.000053"
3. Gage width = 0.00471" ± 0.00012"

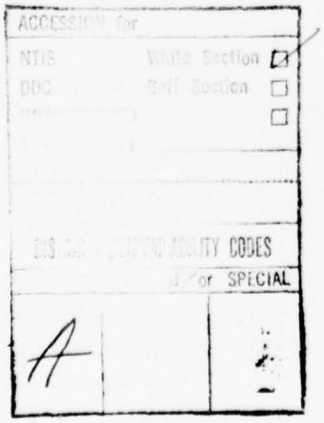

TABLE OF CONTENTS

LIST OF TABLES

LIST OF FIGURES

LIST OF FIGURES
(Continued)

INTRODUCTION

In recent years, solid propellant motor developers have been using embedded stress transducers for monitoring propellant/case bondline stresses in a number of instrumented motors. While useful trends may have been obtained, the accuracy of the measurements was unknown. A major cause for the uncertainty was due to the gage/grain interaction phenomenon. When a rigid transducer is embedded in a solid propellant grain, its presence locally changes the stress and strain patterns produced in the grain by both thermal and mechanical loads. Conversely, any change in propellant mechanical properties, such as the load-history dependent modulus variation inherent in propellant behavior, influences the relationship between the response (output) of the transducer and the "stress at the gage location" (actually, the measurement desired is the stress which would exist at the gage location if the gage were not present). Therefore, to interpret output data from embedded stress transducers, one must account for the gage/grain interaction effects. One method for accomplishing this interpretation is to calculate the quantitative effects under various loading conditions through the application of finite element analysis. To make an accurate calculation, the physical details of the stress transducer's sensitive components must be modelled faithfully. Most of the tranducer physical details can be readily obtained from applicable design drawings or by simple and direct measurements. A major exception is the thickness of the epoxy adhesive layer between the silicon sensing element and and the metal diaphragm (or beam). Current state-of-the-art does not allow scientific control of the epoxy thickness in transducer manufacturing. It is dependent on the artistic skill of the technician and the type of epoxy employed. Furthermore, typical epoxy thickness values of current stress transducers are not available in the literature.

The objective of the work described in this report was to demonstrate the feasibility of using metallurgical grinding and polishing techniques to determine the epoxy layer thickness in a typical semiconductor stress transducer bonding system, and to obtain some typical epoxy bond thickness values for the stress tranducer currently being developed by Chemical Systems Division (CSD) of

United Technologies under AFRPL Contract F04611-75-C-0042. A typical specimen was obtained from Senso-Metrics, CSD's transducer subcontractor, for this purpose. It consisted of two silicon strain gages bonded to a piece of 17-4 stainless steel with an epoxy (Epoxylite 6203).

EXPERIMENTAL PROCEDURES

The basic method used for determining the epoxy bond thickness was to section and polish the specimen at a convenient number of successive planes perpendicular to the length of the bonded silicon gage and photograph the cross-sections. Prior to sectioning, the specimen was studied using a Qwik Scanning Electron Microscope (100-4 Coates & Welter). The specimen was coated with a very light layer of gold (not visible) in order to improve visibility by eliminating any charging effects caused by the non-conducting epoxy. A variety of polaroid photographs were also taken with the KEVEX (Energy dispersive X-ray analyzer) attachment to the Scanning Electron Microscope for elemental analysis of the dust particles on the specimen surface, the epoxy fillet around the silicon gage, and the gage surface. The dust particles were later removed with a freon jet prior to dissecting the specimen.

The specimen was first sectioned, using a metallurgical cutting wheel, into two halves with each containing a complete bonded silicon gage with gold wire leads as shown in Figure 1, which was taken at 10X magnification. One of the two halves was used in this investigation while the other served as a backup. The surface of the silicon gage was covered with red ink from a felt tipped pen prior to encasing the specimen in lucite in order to preclude possible difficulties in distinguishing epoxy from lucite in subsequent photographic analysis of the epoxy bond cross-sections. One end of the encased specimen was then carefully ground in a plane perpendicular to the length of the silicon gage with 120 grit until the first end of the gage was observed. The grit sizes were then decreased gradually until the specimen was finely polished. Grit sizes used were 120, 240, 320, 400, 600, 6 micron diamond, and 1/4 micron diamond powder. The highly polished cross-section of the specimen was photographed at 500X magnification

with a Bausch & Lomb Metallograph and Polaroid 57 film. These grinding, polishing, and photographing procedures were repeated nine times until the gage was completely ground away. The relative positions of the specimen cross-sections that were investigated are shown in Figure 2. The grind time from one cross-section to another with 120 grit was approximately 20 to 30 seconds.

RESULTS AND DISCUSSIONS

Initially, a composite picture of the epoxy bonded silicon gage specimen at 160X magnification was obtained and is shown in Figure 3. It is evident from this figure that there was an epoxy fillet on each side of the gage as expected. It is also evident and somewhat surprising that numerous dust particles were scattered on and near the gage. To investigate these strange dust particles and the epoxy fillet configuration further, higher magnification photographs ranging from 480X to 5,000X were taken at various angles and localities of the specimen as shown in Figures 4 through 13. From these figures, it appeared that the dust particles were loose and were not partially imbedded in the epoxy coated metal surface. This appearance was later confirmed as the particles were readily removed by using a freon jet. All of these photographs show that the height of the epoxy fillet along the sides of the gage varied considerably. This variation appears more pronouncedly at the higher magnifications as shown in Figures 11 and 13. Epoxy filler particles are also observable in the higher magnification photographs. In Figures 8, 9, and 10, the texture of the metal (17-4 stainless) surface is clearly visible. In comparing the metal texture with the sizes of the epoxy filler particles, the metal surface appeared to be relatively smooth.

The elemental composition of two arbitrarily selected dust particles were evaluated by using the Energy Dispersion Elemental Analysis technique. The results are shown in Figure 14 and 15. The large spike represents aluminum and the secondary spike just above 02 represents gold. In Figure 15, a slight amount of titanium is also indicated. These results indicate that the loose dust particles were likely to be either aluminum powder or some compounds of aluminum such as alumina. The small amount of gold detected was from the light

gold coating put on the specimen as mentioned in the previous section of this report. The source of the slight trace of titanium is unknown.

Elemental composition of the epoxy fillet and of the gage surface were also analyzed, and the results are shown in Figures 16 and 17, respectively. In the case of the epoxy fillet, silicon and gold gave the highest peaks, but magnesium, chlorine, calcium and iron were also detected. Since the epoxy contains talc as a filler, the presence of silicon and magnesium should be expected. The iron peak probably came from the steel plate beneath the epoxy. The source for the gold has been mentioned while the source (or sources) for the chlorine and calcium is unknown. In this particular analysis, the scale was amplified in order to detect the elements in lower concentrations. For the gage surface as shown in Figure 17, silicon got the highest peak and the presence of gold and aluminum gave the reduced peaks. The aluminum peak probably came from the dust particles.

Photographs of the ten gage cross-sections investigated are shown in Figure 18 through 27. The location of each cross-section can be readily identified from Figure 2. The dimensions of these photographs were calibrated by photographing a grid with 0.001 inches spacing as shown in Figure 28. In Figures 18 and 19, the metal base, the epoxy adhesive layer, the silicon gage, the gold leadwire and the epoxy wire cover are all clearly visible. It is interesting to note that the gold wire was not in good contact with the gage at cross-section 1; good contact was evident in cross-section 2, however. In Figures 20 through 25, only the metal base, the gage and the epoxy adhesive layer are shown. In Figure 26, the gold leadwire at the other end of the gage is also shown. Figure 27 shows that only some epoxy and the metal base remained after the gage and the gold leadwire had been ground away. From the gage cross-sectional photographs, the epoxy adhesive layer thickness, the gage thickness, and the gage width were measured. The measurements obtained were tabulated and is presented in Table 1. The epoxy and the gage thickness were measured at three points in each cross-section-left side, center, and right side. The gage width was

obtained at the mid plane of the gage cross-section only. The epoxy and gage thickness data were also plotted as a function of gage length as shown in Figures 29 and 30. It is evident that neither the epoxy layer nor the gage has a constant thickness along either the length or the width of the gage. It is also evident that the epoxy layer at the left side of the gage cross-section was thicker than that at the right side. This indicates that the gage was slanted downward to the right, which is also detectable in the cross-sectional photographs. From Figure 30, it appears that the gage was thinner in the middle and thicker at both ends. The average epoxy thickness was found to be $0.000498 \pm .000067$ inches, while the average gage thickness was found to be 0.000449 ± 0.000053 inches. The composite thickness of epoxy and gage is shown in Figure 31. It can be seen from this figure that the left side was thicker than the right side; thus further indicates that the gage was slanted downward to the right. Figure 31 also indicates that the gage was slanted downward lengthwise toward cross-section 9. The thickness of the composite was also uneven which may be in part due to the unevenness of the metal base surface.

The gage width for the cross-sections investigated are presented graphically in Figure 32. It is seen that the gage was narrower at the middle than at either end. The average gage width was found to be 0.00471 ± 0.00012 inches, or the width of the gage was a little more than ten times its thickness.

There was a possibility that the variations of gage thickness, gage width and epoxy thickness from cross-section to cross-section were due to unintentional magnification changes in the photographic investigation. To study this possibility, the ratio of gage width to gage thickness for each cross-section was calculated and the results were tabulated in Table 2 and plotted in Figure 33. It is obvious from this figure that this ratio is not a constant from cross-section to cross-section. This clearly indicates that magnification changes, if any, were not an influencing factor in the photographic results.

Other results of interest are that the gage cross-section was found to be of a slight trapezoidal shape with the bottom surface slightly curved upward (bow shaped). These can be readily detected from Figures 20 through 26. It can also

be seen from these figures that the height of the epoxy fillets along the two sides of the gage were uneven. It is very apparent that the fillet on the right side was much higher. This variation, along with the results presented earlier that the gage was slanted downward to the right, tend to infer that the gage was placed on the epoxy layer with higher pressure applied to the right side.

CONCLUSIONS AND RECOMMENDATIONS

1. The feasibility of using metallurgical grinding and polishing techniques for determining the thickness of the epoxy adhesive in a silicon gage bonding system was demonstrated.

2. For the specimen investigated, the following quantities were determined:
   (1) Average epoxy layer thickness = 0.000498" $\pm$ 0.000067".
   (2) Average gage thickness = 0.000449" $\pm$ 0.000053".
   (3) Average gage width = 0.00471" $\pm$ 0.00012".

3. The gage did not have a shape of a respectable rectangular bar and its surfaces were irregular. This quality of gages would not be suitable for molecular (electrostatic field assisted) bonding.

4. Current gaging technique does not provide for good control of epoxy adhesive thickness and epoxy fillet size along the sides of the gage. Improvement in this technique is recommended.

5. The experimental technique demonstrated in this effort is also useful for investigating some potential stress transducer manufacturing problems related to diaphragm surface texture, epoxy filler particle size and silicon/leadwire contact.

6. The dust particles found on the specimen were large in comparison to the thickness of the epoxy adhesive layer. Therefore, gaging should always be done in a dust free environment.

Table 1. Summary of Measured Specimen Data

Cross-Section No.	Epoxy Thickness, In. X 10^{-3}			Gage Thickness, In. X 10^{-3}			Gage Width, In. X 10^{-3}
	Left	Center	Right	Left	Center	Right	
1	0.680	0.500	0.540	0.440	0.480	0.480	4.88
2	0.520	0.480	0.420	0.480	0.560	0.580	4.86
3	0.500	0.480	0.400	0.480	0.520	0.520	4.80
4	0.520	0.480	0.440	0.440	0.440	0.420	4.72
5	0.580	0.540	0.520	0.400	0.440	0.400	4.66
6	0.600	0.540	0.500	0.340	0.420	0.380	4.60
7	0.540	0.460	0.420	0.420	0.440	0.440	4.72
8	0.540	0.400	0.440	0.440	0.460	0.460	4.72
9	0.560	0.400	0.440	0.400	0.400	0.440	4.84
10	---	---	---	0	0	0	0
Average	0.560±	0.476±	0.460±	0.427±	0.462±	0.458±	4.71±
	0.055	0.051	0.040	0.044	0.050	0.062	0.12
Overall Average	0.498 ± 0.067			0.449 ± 0.053			

Table 2. Ratios of Gage Width to Gage Thickness

Cross-Section No.	Width to Thickness Ratio		
	Left	Center	Right
1	11.09	10.17	10.17
2	10.13	8.68	8.38
3	10.00	9.23	9.23
4	10.73	10.73	11.24
5	11.65	10.59	11.65
6	13.53	10.95	12.11
7	11.24	10.73	10.73
8	10.73	10.26	10.26
9	12.10	12.10	11.00

Average ratio = 10.72
Standard deviation = 1.11
Percent deviation = 10.4%

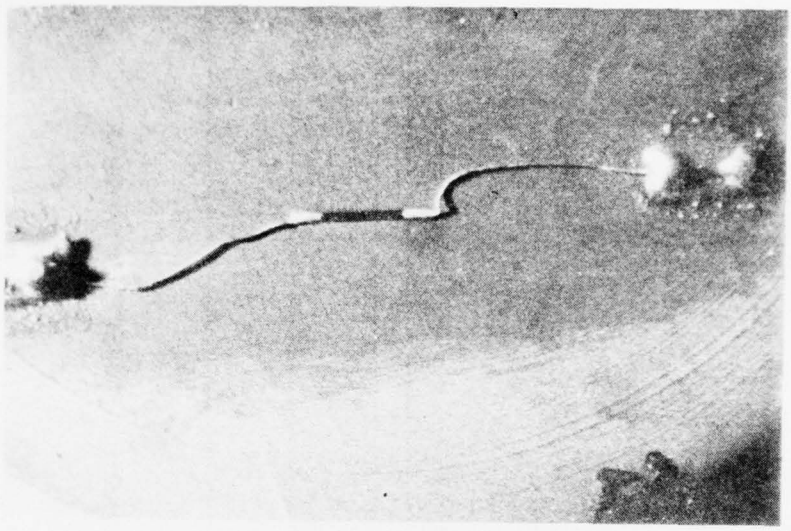

Figure 1. Epoxy Bonded Silicon Gage Specimen (10X)

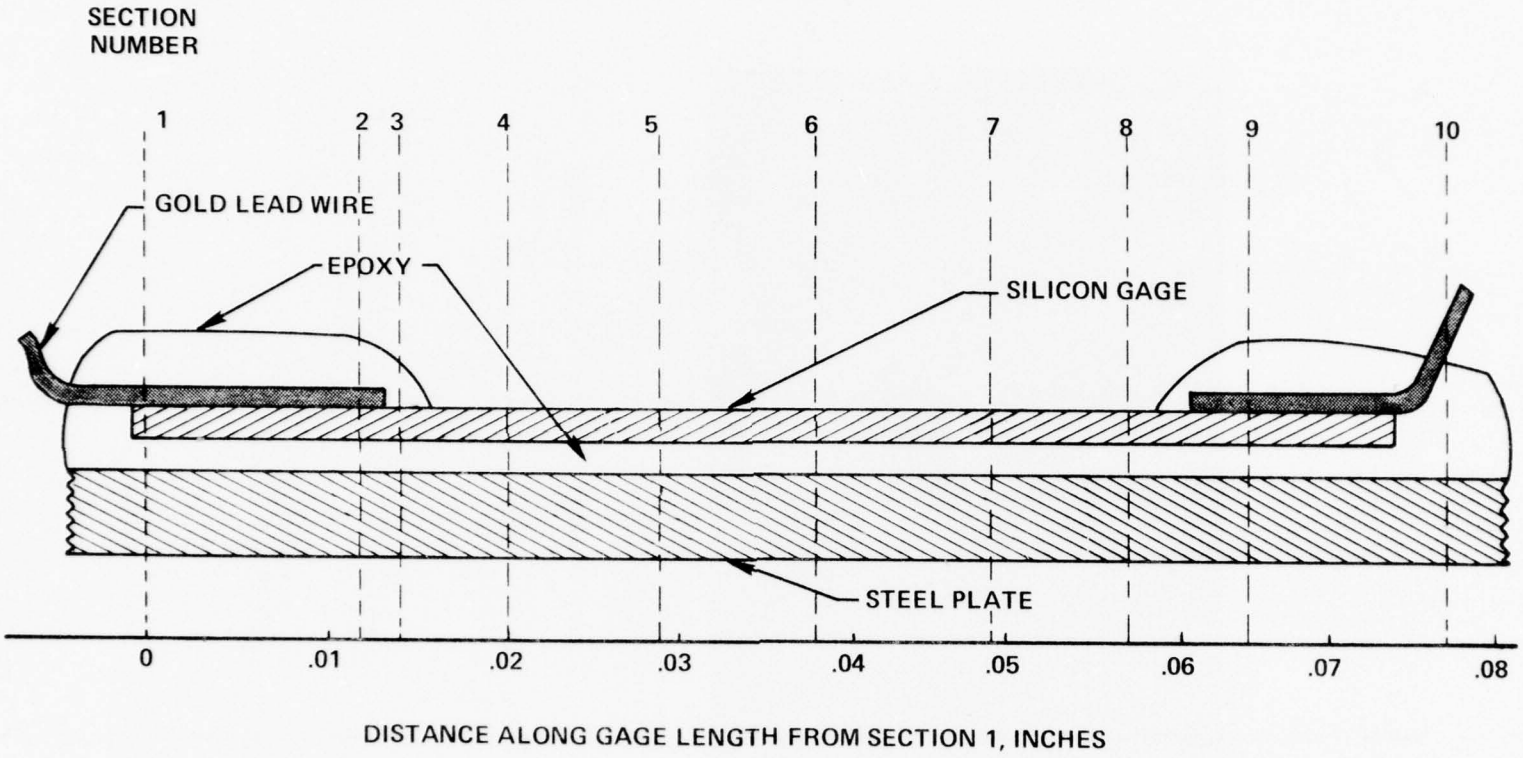

Figure 2. Sections of Bonded Silicon Strain Gage Investigated

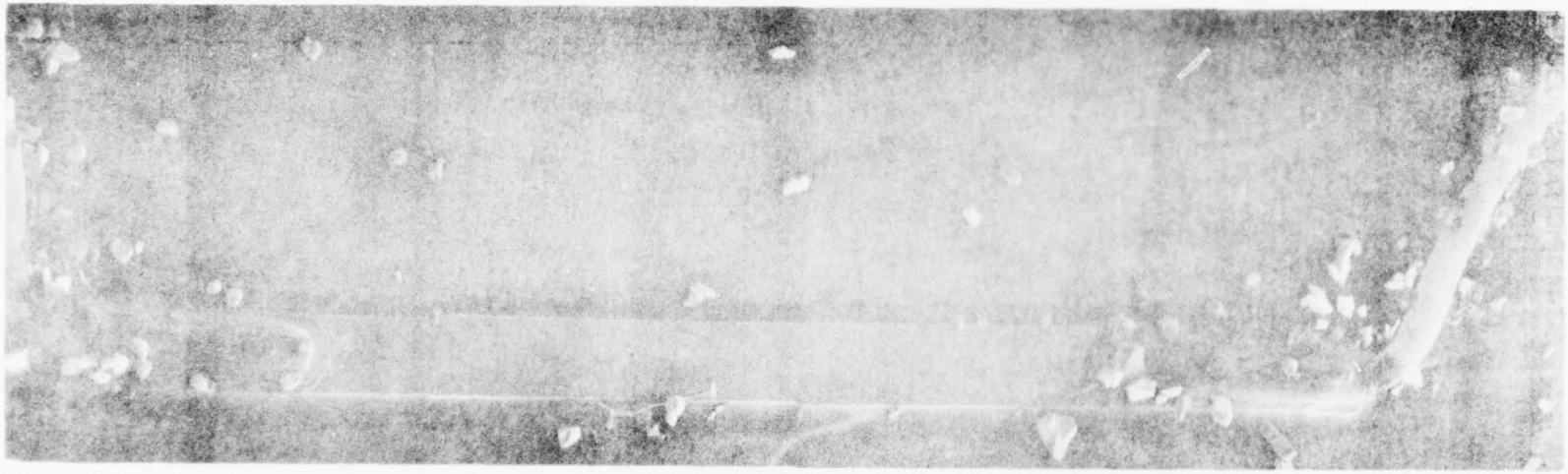

Figure 3. Composite Picture of One Bonded Silicon Strain Gage with Gold Lead Attachment (160X)

Figure 4. Lead Attachment Area (1,600X)

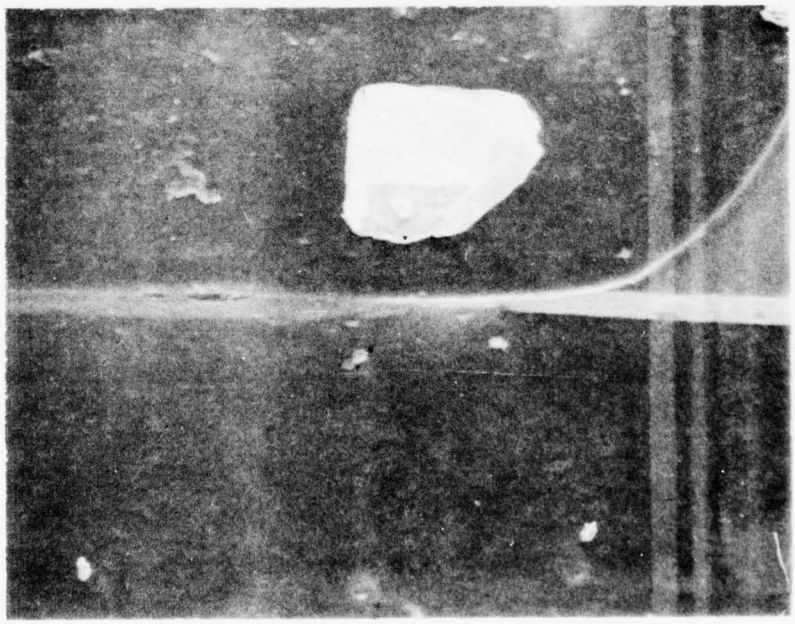

Figure 5. Lead Attachment Area (1,100X)

Figure 6. Side of Bonded Silicon Gage (2, 200X)

Figure 7. Side of Bonded Silicon Gage (2, 200X)

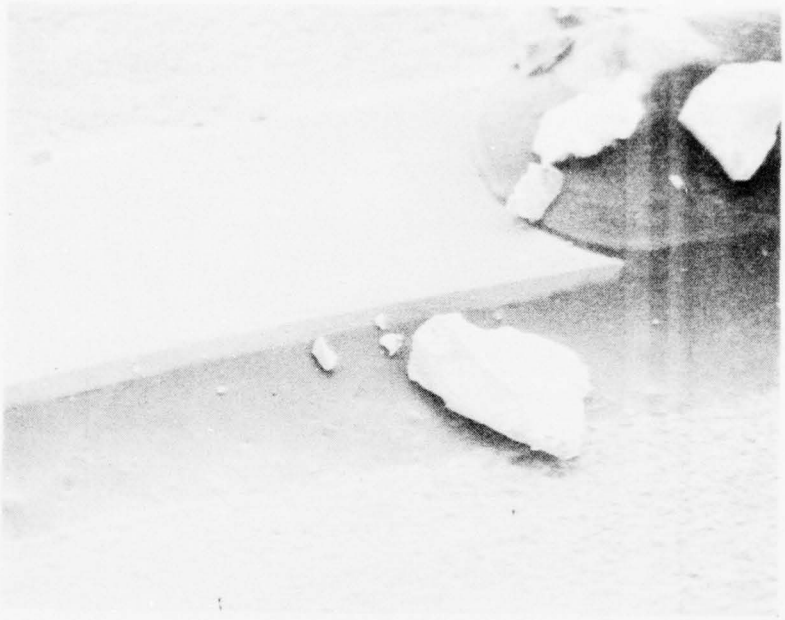

Figure 8. Lead Attachment Area (480X)

Figure 9. Side of Bonded Silicon Gage (650X)

Figure 10. Side Edge of Bonded Silicon Gage (1,200X)

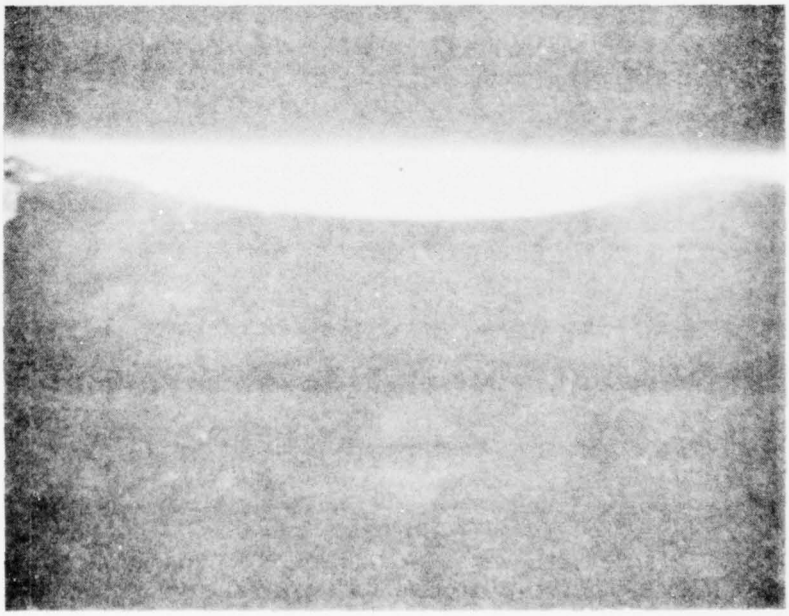

Figure 11. Side of Bonded Silicon Gage (5,000X)

Figure 12. Side of Bonded Silicon Gage (3,400X)

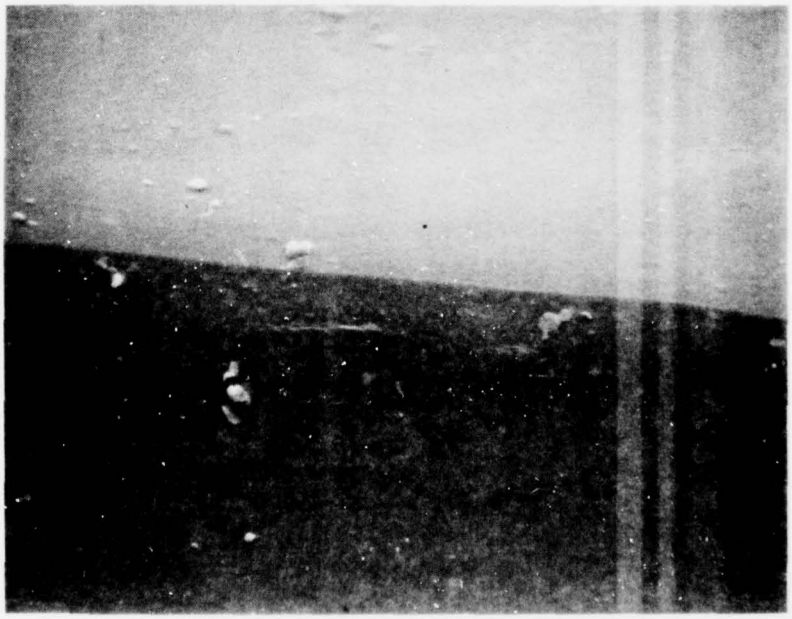

Figure 13. Side of Bonded Silicon Gage (1,600X)

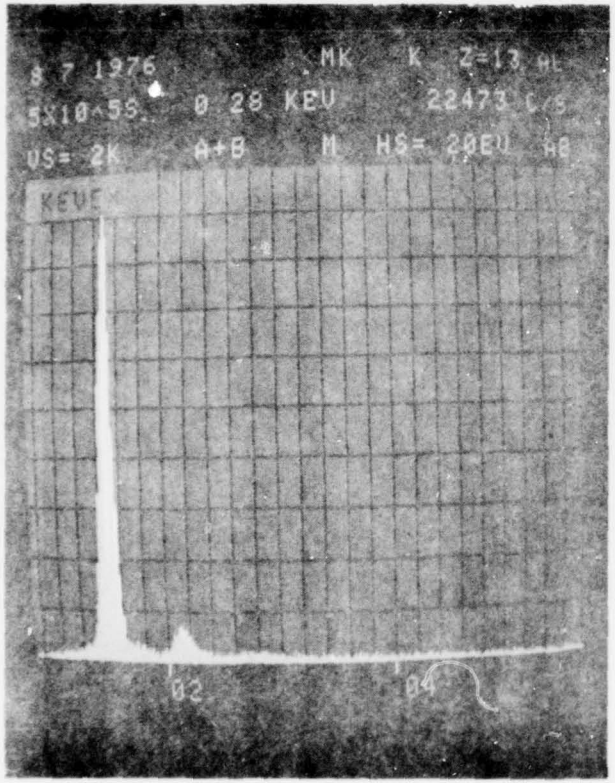

Figure 14. Elemental Analysis of a Dust Particle

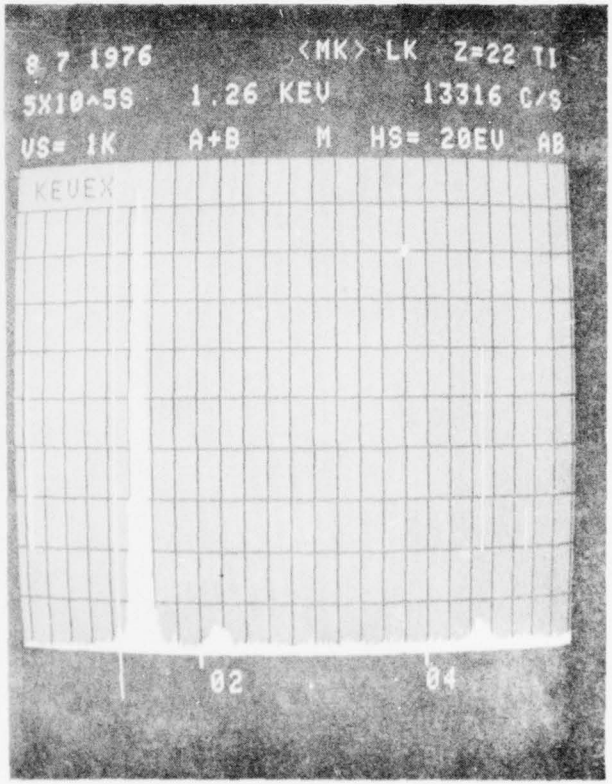

Figure 15. Elemental Analysis of a Second Dust Particle

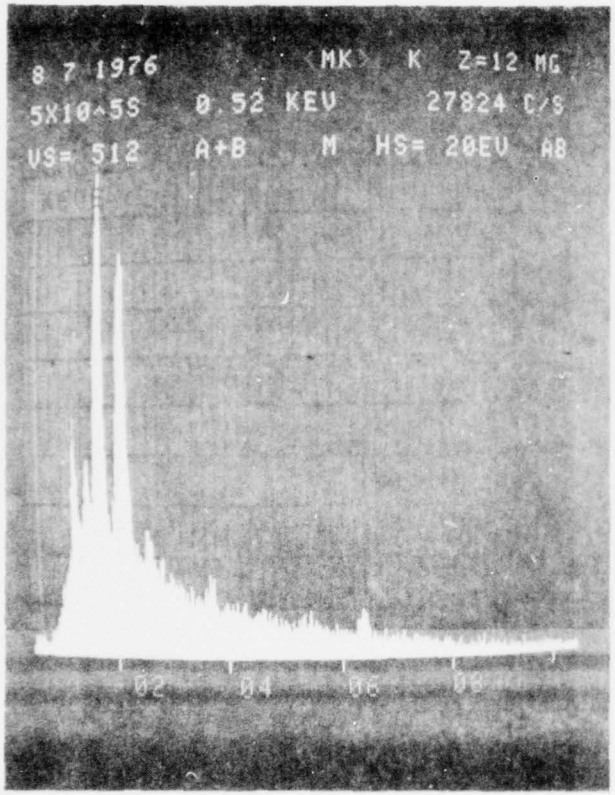

Figure 16. Elemental Analysis of Epoxy Fillet

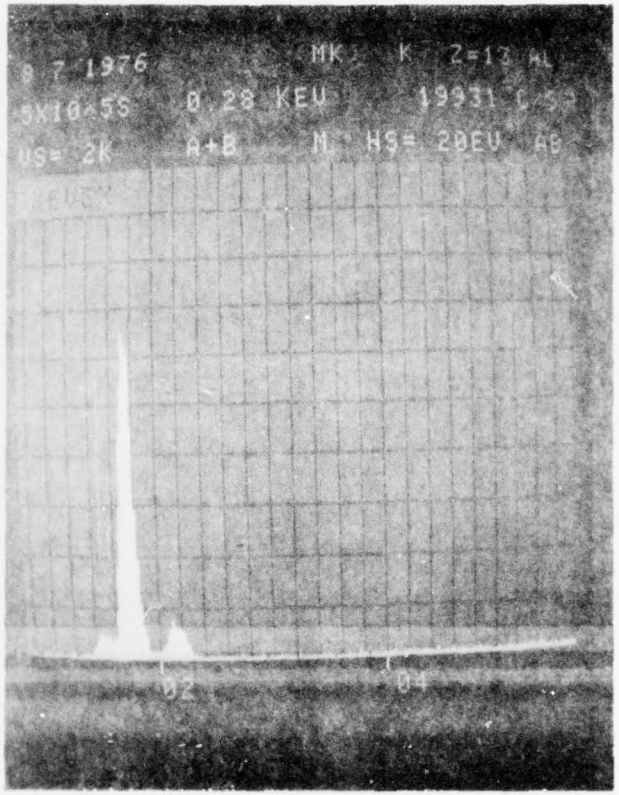

Figure 17. Elemental Analysis of Silicon Gage Surface

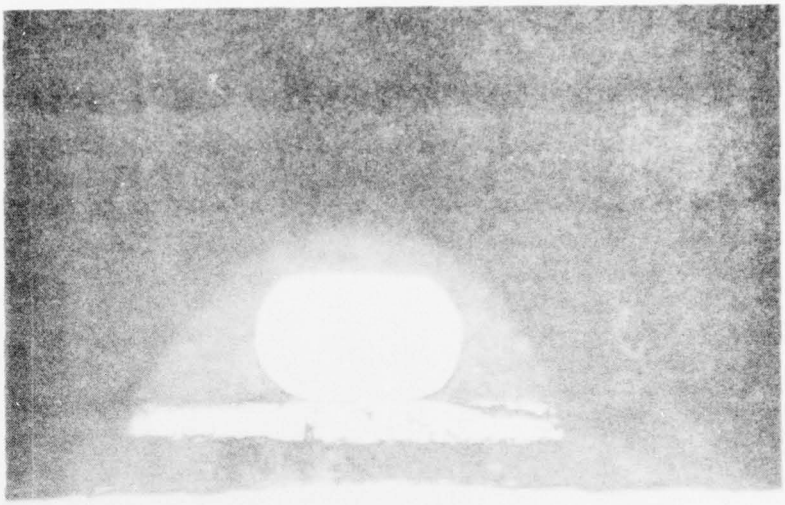

Figure 18. Specimen Cross-Section 1 (500X)

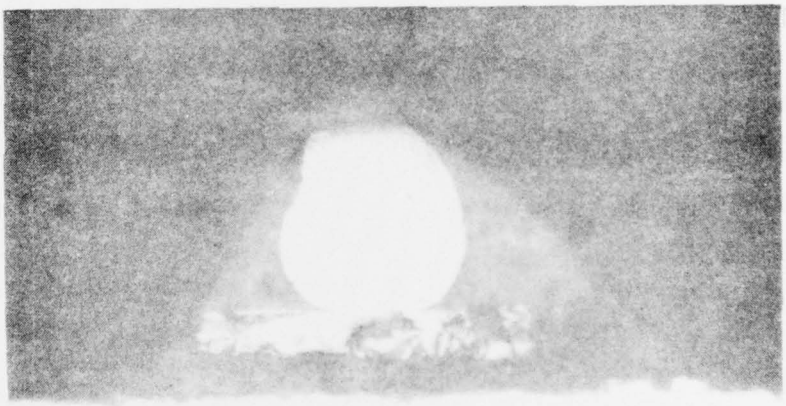

Figure 19. Specimen Cross-Section 2 (500X)

Figure 20. Specimen Cross-Section 3 (500X)

Figure 21. Specimen Cross-Section 4 (500X)

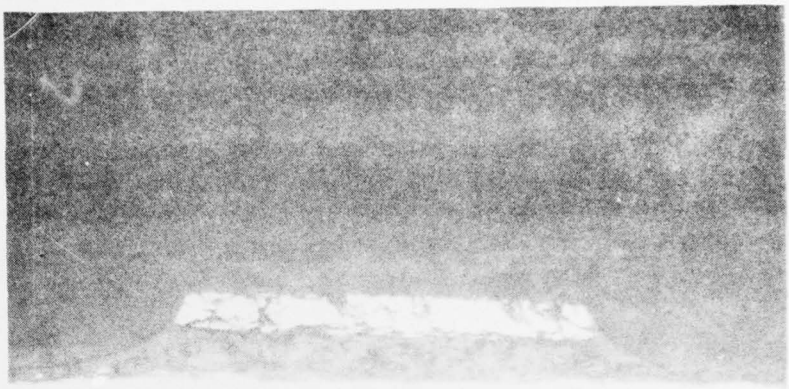

Figure 22. Specimen Cross-Section 5 (500X)

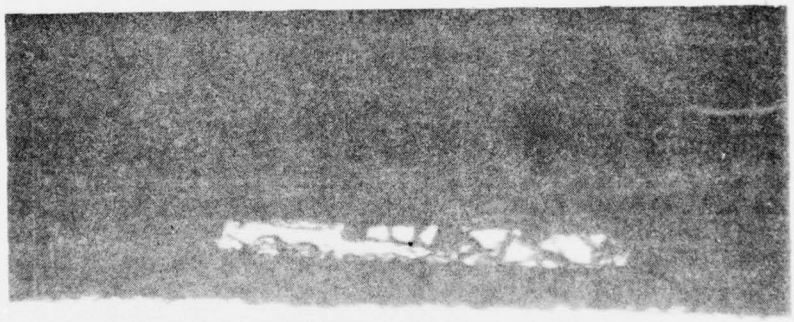

Figure 23. Specimen Cross-Section 6 (500X)

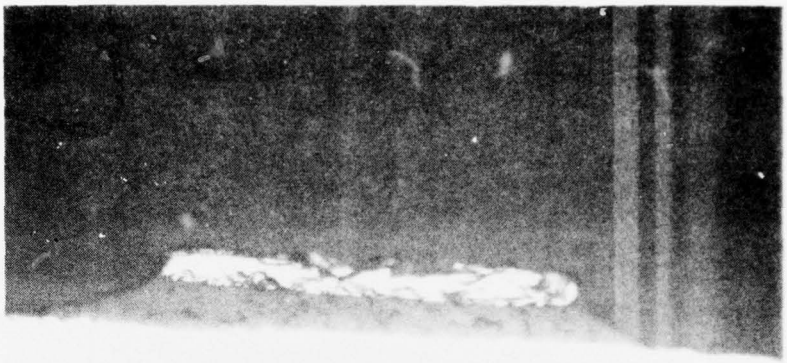

Figure 24. Specimen Cross-Section 7 (500X)

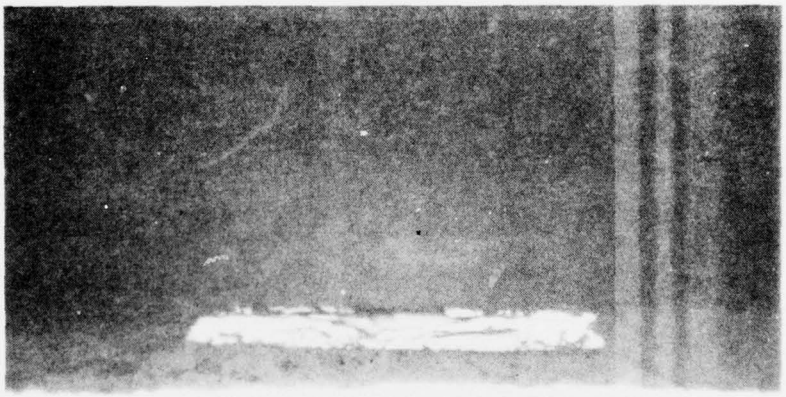

Figure 25. Specimen Cross-Section 8 (500X)

Figure 26. Specimen Cross-Section 9 (500X)

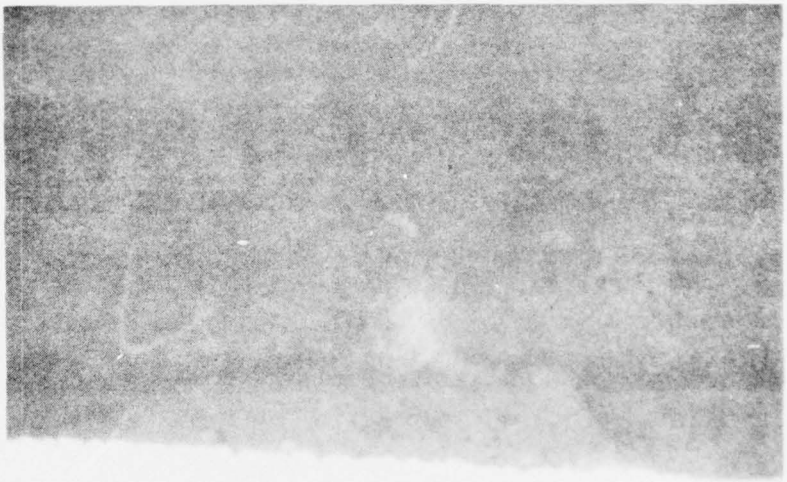

Figure 27. Specimen Cross-Section 10 (500X)

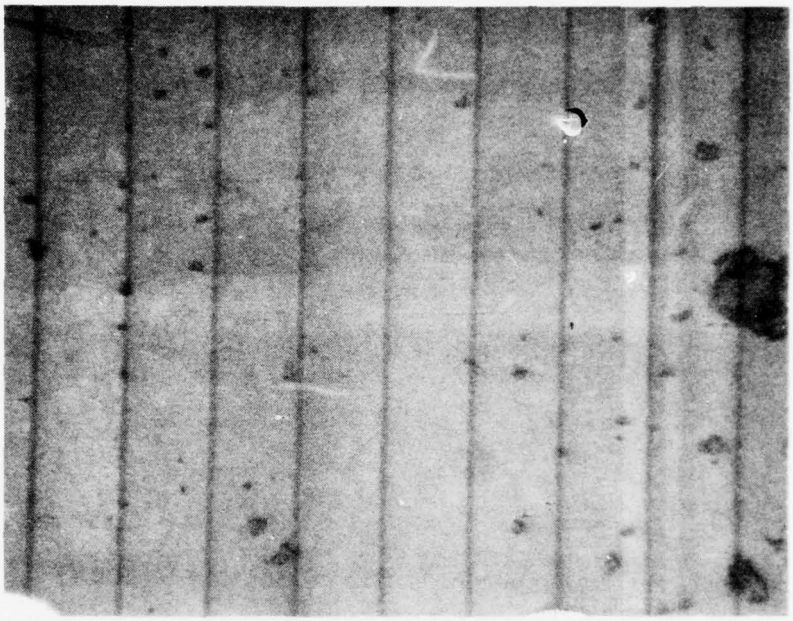

Figure 28. Calibration Photograph of 0.001" Grid (500X)

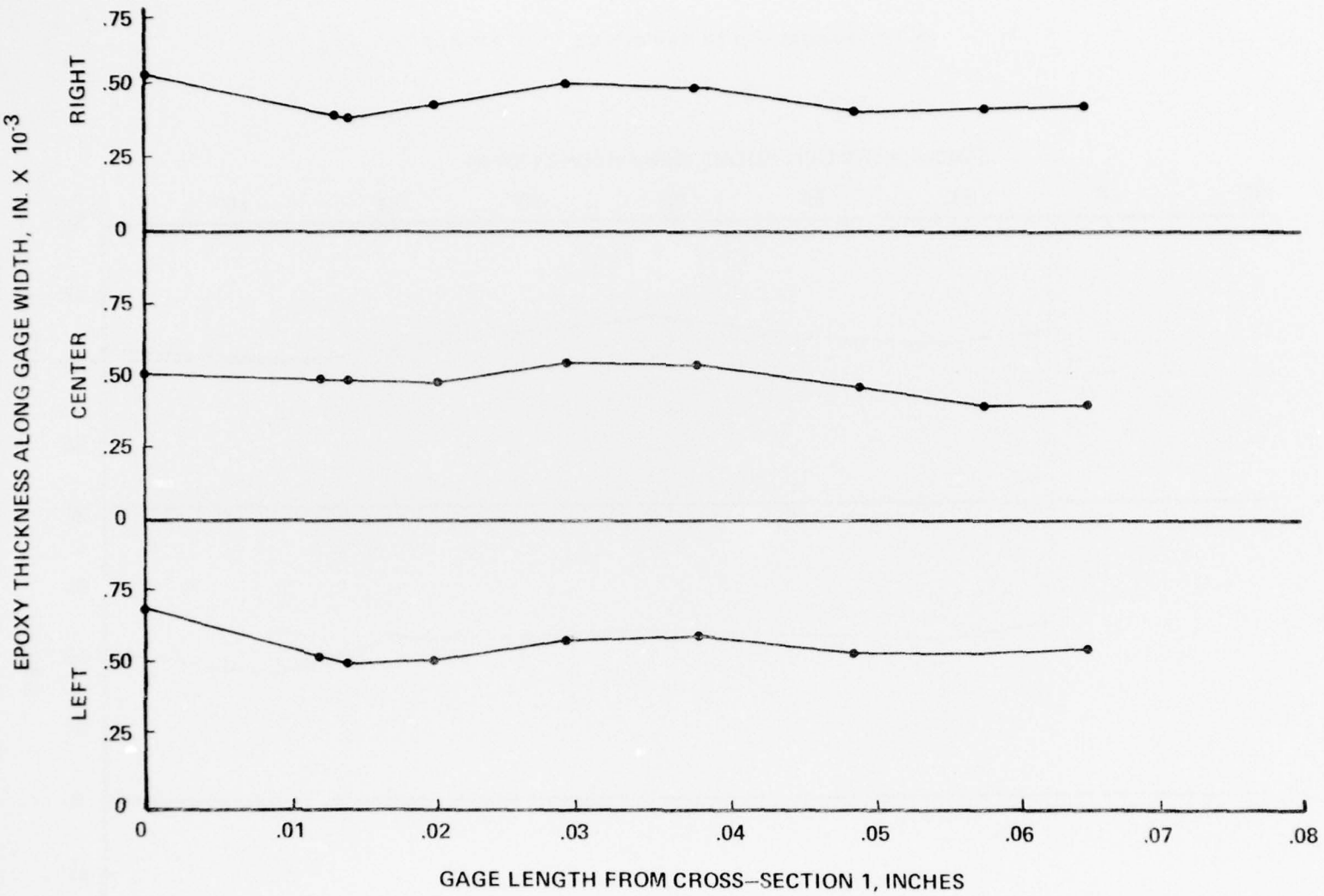

Figure 29. Thickness of the Epoxy Adhesive Layer

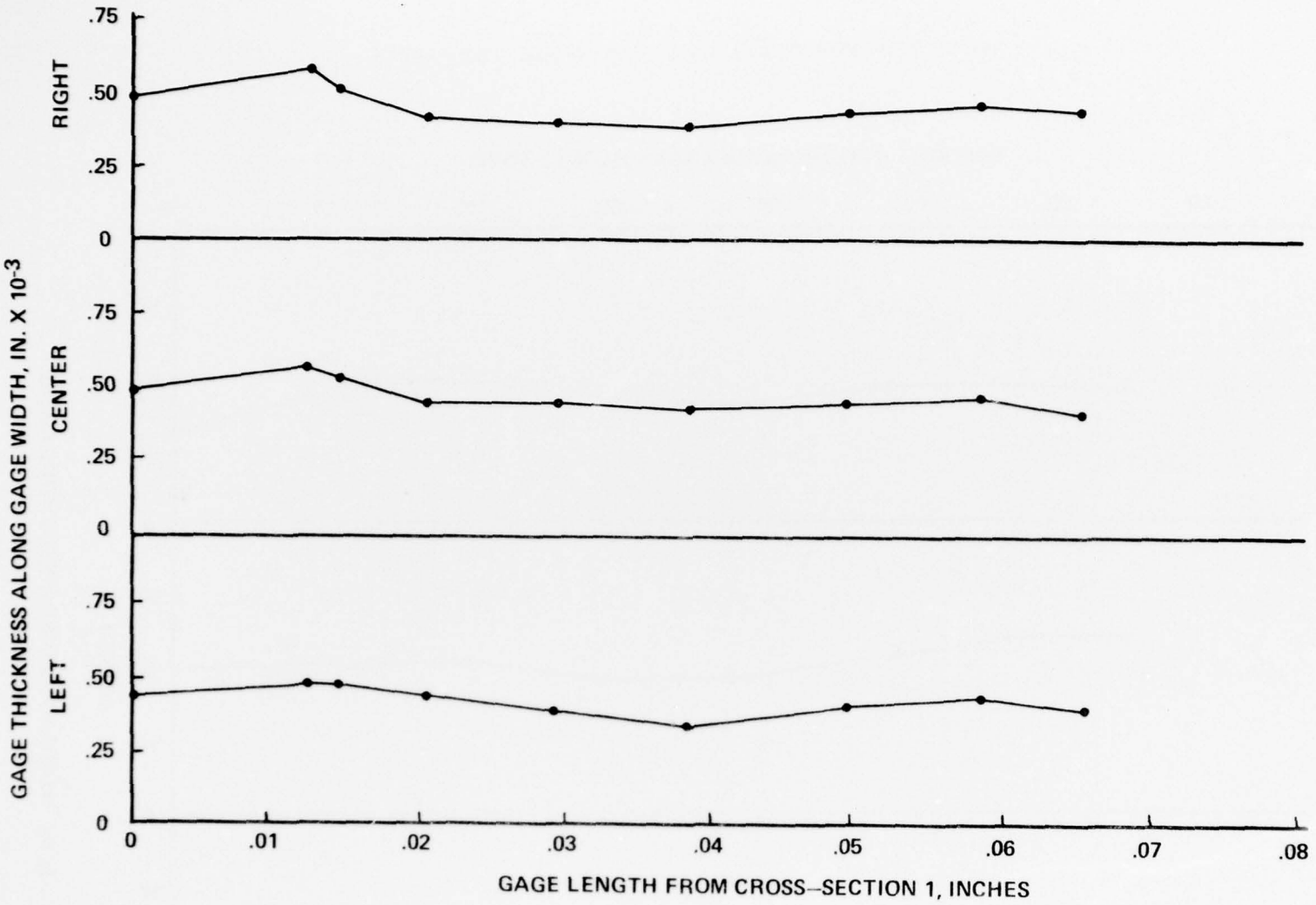

Figure 30. Thickness of the Silicon Gage

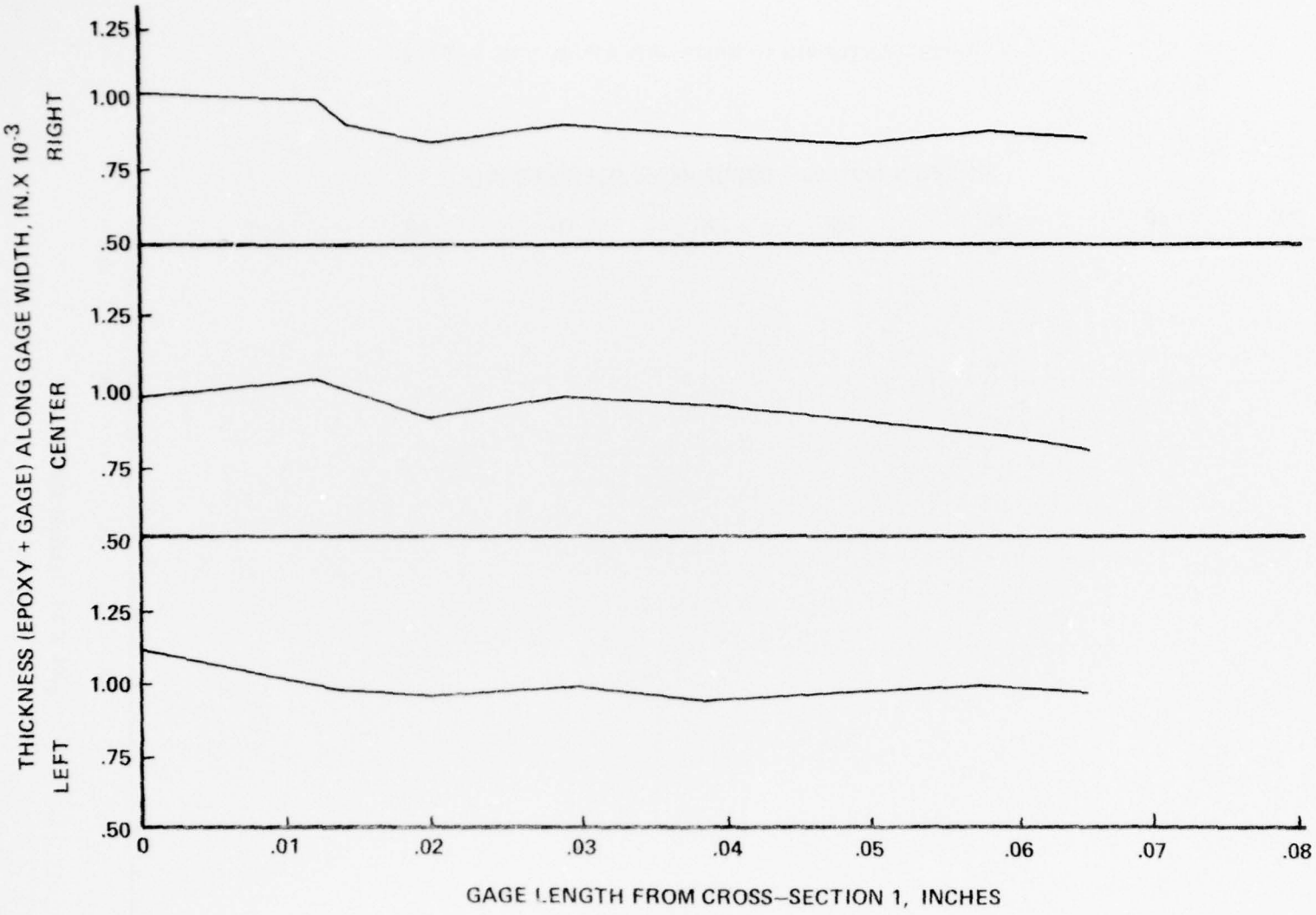

Figure 31. Composite Thickness of Epoxy Adhesive Layer and Silicon Gage

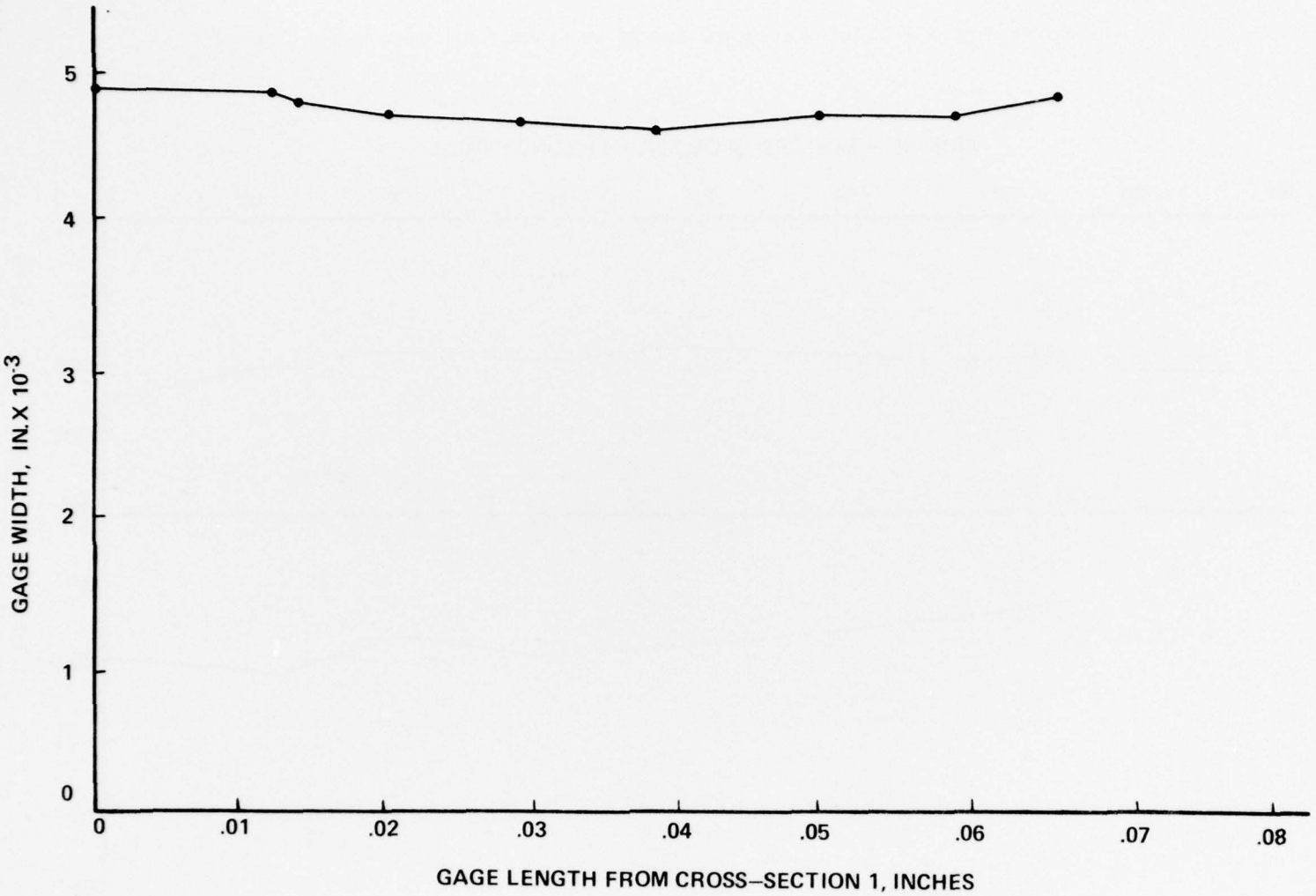

Figure 32. Width Variation of the Silicon Gage

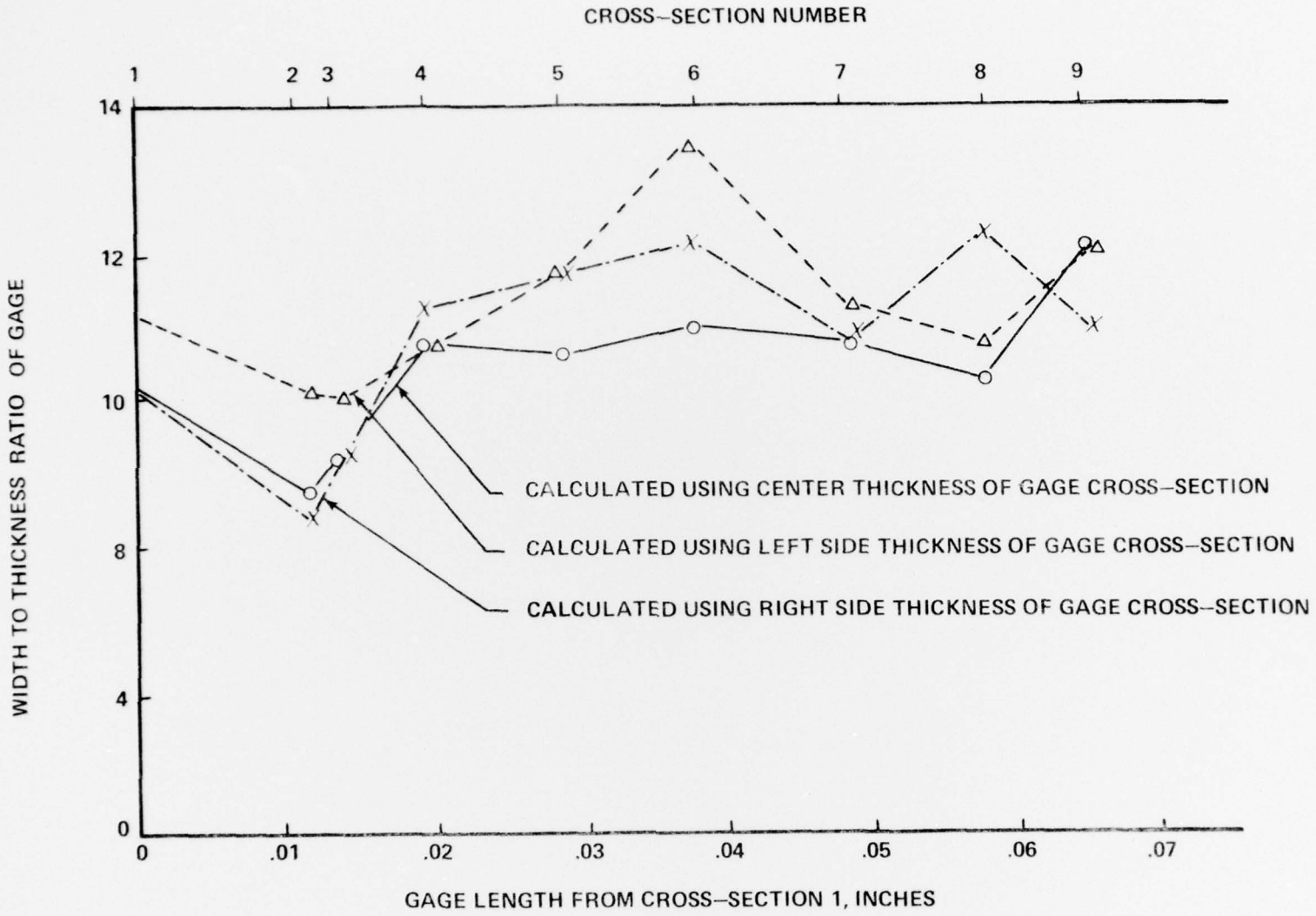

Figure 33. Variation of the Gage Width to Gage Thickness Ratio